Ferrocyanide–Ferricyanide Redox Couple Induced Electrochemiluminescence Amplification of Carbon Dots for Ultrasensitive Sensing of Glutathione

ARTICLE *in* ANALYTICAL CHEMISTRY · OCTOBER 2015

Impact Factor: 5.64 · DOI: 10.1021/acs.analchem.5b03358

5 AUTHORS, INCLUDING:

Serge Cosnier

French National Centre for Scientific Research

346 PUBLICATIONS **9,665** CITATIONS

SEE PROFILE

Dan Shan

Nanjing University of Science and Technology

88 PUBLICATIONS **2,097** CITATIONS

SEE PROFILE

analytical chemistry

Article

pubs.acs.org/ac

Ferrocyanide-Ferricyanide Redox Couple Induced Electrochemiluminescence Amplification of Carbon Dots for Ultrasensitive Sensing of Glutathione

Wen-Jun Niu,[†] Rong-Hui Zhu,[†] Serge Cosnier,[‡] Xue-Ji Zhang,[†] and Dan Shan*[,†]

[†]Sino-French Laboratory of Biomaterials and Bioanalytical Chemistry, School of Environmental and Biological Engineering, Nanjing University of Science and Technology, Nanjing, Jiangsu Province 210094, China

[‡]University of Grenoble Alpes-CNRS, DCM UMR 5250, F-38000 Grenoble, France

ABSTRACT: Here we report a novel solid-state ECL sensor for ultrasensitive sensing of glutathione (GSH) based on ferrocyanide-ferricyanide redox couple ($Fe(CN)_6^{3-/4-}$) induced electrochemiluminescence (ECL) amplification of carbon dots (C-dots). The electropolymerization of C-dots and (11-pyrrolyl-1-yl-undecyl) triethylammonium tetrafluoroborate (A_2) enabled immobilization of the hydrophilic C-dots on the surface of glassy carbon electrode (GCE) perfectly, while the excellent conductivity of polypyrrole was exploited to accelerate electron transfer between them. The $Fe(CN)_6^{3-/4-}$ can expeditiously convert the C-dots and $S_2O_8^{2-}$ to C-dot$^{\bullet-}$ and $SO_4^{\bullet-}$, respectively. High yields of the excited state C-dots (C-dots*) were obtained, and a ~10-fold ECL amplification was realized. The C-dots* obtained through the recombination of electron-injected and hole-injected processes may be impeded due to the interference of GSH to $K_2S_2O_8$. Therefore, the constructed sensor for GSH showed a detection limit down to 54.3 nM (S/N = 3) and a wide linear range from 0.1−1.0 μM with a correlation coefficient of 0.997.

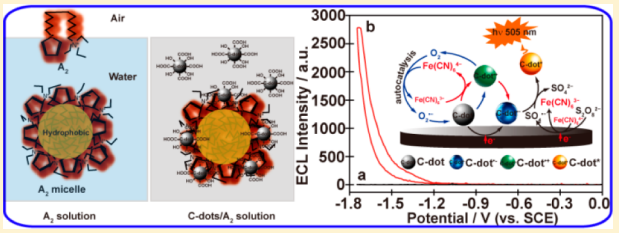

Carbon dots (C-dots), as a new emerging type of luminescent nanomaterials, have drawn increasing attention in recent years owing to their excellent chemical inertness,[1,2] fascinating optical properties,[3−6] favorable biocompatibility,[7−10] and, more importantly, their unique electrochemiluminescence (ECL) characters.[11−16] Accordingly, C-dots have become promising alternatives to traditional ECL luminophores such as $Ru(bpy)_3^{2+}$,[17,18] noble metal nanoclusters,[19,20] and quantum dots (QDs).[21−24] However, so far as we know, there are only a few reports on the use of C-dots in ECL compared with a considerable number of investigations on QDs ECL systems. One possible reason is that the preparation of C-dots still involves expensive precursors and intricate processes and often giving C-dots with broad size distributions and low quantum yields (QY). The other main reason is that C-dots in ECL are still at an early stage; the detailed reasons and rules for ECL generation have not yet been explored thoroughly and systematically compared to QDs, for example.

As we know, ECL is chemiluminescence triggered by electrochemical processes, which combines the advantages of chemiluminescent analysis with electrochemical analysis. Therefore, it exhibits ultrasensitive sensing with a wide response range.[21,25] Nevertheless, as reported by the literature elsewhere, the hydrophilic C-dots have been scarcely immobilized on the surface of glassy carbon electrode (GCE) without surface modification with chitosan, naphthol, and so on.[26−28] The poor conductivity of GCE modified with chitosan or naphthol may impede the electron transfer on the electrode surface. As a result, C-dots in ECL systems always present narrow potential windows and weak ECL signals. To overcome these limitations, carbon-based nanomaterials including carbon nanotubes (CNTs) and graphene sheets were usually selected to improve the ECL systems because of their outstanding electric conductivity.[29−32] Although the ECL intensity was enhanced, intricate processes were usually involved. In addition, to our knowledge, the ferrocyanide-ferricyanide redox system ($Fe(CN)_6^{3-/4-}$) can serve as the electron injector and hole injector in a series of possible reactions, which accelerates electrons transfer in electrochemical reactions.[33,34] However, the $Fe(CN)_6^{3-/4-}$ in solutions would destroy the buffer condition and could even oxidize all of the analytes, making the sensor systems lose selectivity and biocompatibility.

Moreover, glutathione (GSH) is an essential endogenous antioxidant in cellular systems for defense against toxins and free radicals, which is ubiquitous in mammalian and many prokaryotic cells.[35] Abnormal levels of GSH are directly related to slow growth in children, psoriasis, hair depigmentation, cellular and organ damage, and even some diseases such as cancer, AIDS, Alzheimer's, diabetes mellitus, cardiovascular disease, and others.[36] Therefore, it is very significant and essential to develop a simple and sensitive strategy for the determination of GSH.

Herein, in this paper, we report a novel solid-state ECL sensing strategy based on $Fe(CN)_6^{3-/4-}$ induced ECL

Received: September 3, 2015
Accepted: October 19, 2015

DOI: 10.1021/acs.analchem.5b03358
Anal. Chem. XXXX, XXX, XXX−XXX

amplification of C-dots systems. Specifically, (11-pyrrolyl-1-yl-undecyl) triethylammonium tetrafluoroborate (A_2) is a kind of cationic surfactant, which can be clutched firmly with the negative C-dots through electrostatic interactions. Then, as one of the pyrrole derivatives, C-dots/A_2 can be electrochemically polymerized to poly(C-dots/A_2) consecutively, while the excellent conductivity of polypyrrole can accelerate electron transfer on the electrode surface. After that, the solid-state ECL sensor is constructed using electrochemically confined Fe-$(CN)_6^{3-/4-}$ on the surface of poly(C-dots/A_2) to enhance ECL signals. Finally, the mechanism of $Fe(CN)_6^{3-/4-}$ amplified ECL of the C-dots system is proposed, and the ECL platform is applied for the sensitive and selective detection of GSH in the presence of other interfering substances.

EXPERIMENTAL SECTION

Reagents and Materials. (11-Pyrrolyl-1-yl-undecyl) triethylammonium tetrafluoroborate (A_2) was synthesized according to the previously described protocol.[33] Alanine (Ala), histidine (His), cysteine (Cys), ethylenediamine, glutathione (GSH), glutamic acid, ascorbic acid, asparagic acid, folic acid, dopamine, methionine, tryptophan, valine, and vitamin B_1/B_2/B_6 were purchased from J&K Scientific Inc. (Shanghai, China). All other chemicals were of analytical grade and used without further purification. Phosphate buffer solution (PBS) containing 0.1 M K_2HPO_4 and KH_2PO_4 was used as the electrolyte in cyclic voltammetric analysis. Tris-HCl buffer solution (0.05 M, pH 7.4) containing 10 mM $K_2S_2O_8$ and 0.1 M KCl was used as the electrolyte in ECL analysis. Double-distilled water was used throughout the experiment.

Measurements and Apparatus. A CHI 660D electrochemical workstation (CH Instrument) was used for cyclic voltammetry (CV) measurements. All electrochemical studies were performed with a conventional three electrode system. A saturated calomel electrode (SCE) and a Pt wire electrode were used as reference and counter electrodes, respectively. All the potentials mentioned below are relative to SCE. The working electrode was a glassy carbon electrode (GCE) (diameter 5 mm) polished carefully with 0.05 μm alumina particles on polishing cloth before use. The morphology of the modified electrodes was investigated with a field emission scanning electron microscopy (S-4800 FE-SEM, Hitachi, Japan). ECL measurements were carried out using a MPI-EII multifunctional electrochemical and chemiluminescent analytical system (Xi'an Remex Analytical Instrument Co., Ltd., China). ECL spectra were collected with an Edinburgh FLS920 fluorescence spectrometer (Livingston, UK).

Preparation of C-Dots. The C-dots were prepared by a hydrothermal carbonization protocol reported previously.[37] Briefly, 2.673 g of alanine was dissolved into 30.0 mL of ultrapure water, followed by addition of 500 μL of ethylenediamine under stirring. Then, the solution was transferred into a Teflon-lined autoclave (50.0 mL) and heated to 200 °C for 6 h. After that, the chamber was cooled to room temperature. The product, which was brown-black and transparent, was dialyzed in a dialysis bag (1000 MWCO) for 24 h. Finally, the mixture was dried by rotary evaporator at 45 °C to obtain solid powders for further use.

Immobilization of C-Dots on the Surface of GCE. The pyrrole-tethered cationic surfactant, A_2, was dispersed in double-distilled water under sonication with a concentration of 8 mM. The C-dots/A_2 composite (2.5 mg/mL) was obtained by mixing the as-prepared C-dots to the A_2 solution with sonication for 10 min. GCE/PolyA_2 and GCE/poly(C-dots/A_2) were prepared by coating GCE with 10 μL of A_2 and C-dots/A_2 dispersion, respectively, and subsequent drying at room temperature for 30 min. The modified electrodes were then transferred into an electrochemical cell containing aqueous 0.1 M $LiClO_4$, and the coatings were electropolymerized by cyclic voltammetry between 0 to 0.9 V for 80 cycles at a scan rate of 50 mV s^{-1}.

Preparation of GCE/Poly(C-dots/A_2)-Fe$(CN)_6^{3-/4-}$. The GCE/poly(C-dots/A_2) was dipped into 0.1 M PBS (pH 7.0) containing 10 mM $K_3Fe(CN)_6$/$K_4Fe(CN)_6$ (1:1) and scanned by cyclic voltammetry between −0.4 to 0.7 V for 60 cycles at a scan rate of 50 mV s^{-1}. Subsequently, the modified electrode was washed thoroughly with double-distilled water for further characterization and use. In a similar way, poly(C-dots/A_2)-$Fe(CN)_6^{4-}$and poly(C-dots/A_2)-$Fe(CN)_6^{3-}$ modified GCE were prepared as well.

RESULTS

Electrochemical Investigation. As mentioned above, the confined $Fe(CN)_6^{3-/4-}$ was achieved by dipping GCE/poly(C-dots/A_2) into 0.1 M PBS (pH 7.0) containing 10 mM $K_3Fe(CN)_6$/$K_4Fe(CN)_6$ (1:1) and scanned between −0.4−0.7 V for 60 cycles at a scan rate of 50 mV s^{-1}. Cyclic voltammetry (CV) was used to investigate the electrochemical behaviors of the confined $Fe(CN)_6^{3-/4-}$ in the poly(C-dots/A_2) system. At the bare GCE (Figure 1A, curve a), the CV of $Fe(CN)_6^{3-/4-}$ exhibits a pair of redox peaks, with the anodic peak potential

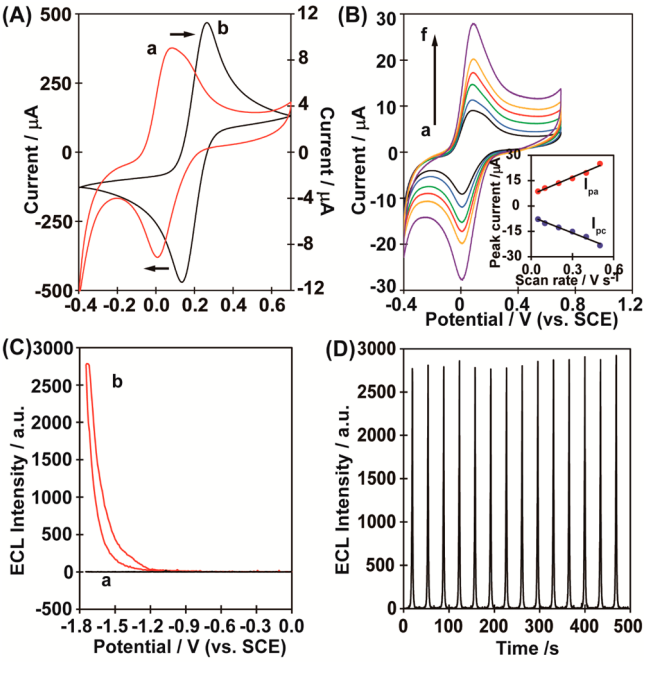

Figure 1. (**A**) CVs of GCE obtained in 0.1 M PBS (pH 7.0) containing 10 mM $K_4Fe(CN)_6$/$K_3Fe(CN)_6$ (a) and poly(C-dots/A_2)-$Fe(CN)_6^{3-/4-}$ in 0.1 M PBS (pH 7.0) (b) at a scan rate of 50 mV s^{-1}, respectively. (**B**) CVs of poly(C-dots/A_2)-$Fe(CN)_6^{3-/4-}$ in 0.1 M PBS (pH 7.0) at various scan rates. The scan rate from inner to outer is 50 (a), 100 (b), 200 (c), 300 (d), 400 (e), and 500 mV s^{-1} (f). Inset: Plots of anodic and cathodic peak currents vs scan rates. (**C**) ECL-potential curves of poly(C-dots/A_2)-$Fe(CN)_6^{3-/4-}$ in 0.05 M Tirs-HCl (pH 7.4) without (a) and with (b) 10 mM $K_2S_2O_8$ at a scan rate of 100 mV s^{-1}. (**D**) ECL responses of poly(C-dots/A_2)-$Fe(CN)_6^{3-/4-}$ obtained during a continuous potential scan between −1.75 and 0 V.

DOI: 10.1021/acs.analchem.5b03358
Anal. Chem. XXXX, XXX, XXX−XXX

(E_{pa}) at 264 mV and the cathodic peak potential (E_{pc}) at 133 mV in 0.1 M PBS (pH 7.0). The peak-to-peak separation (ΔE_p) is 131 mV. The formal peak potential ($E^{0\prime}$, the midpoint of E_{pa} and E_{pc}) is around 198 mV. However, for the $Fe(CN)_6^{3-/4-}$ entrapped in the poly(C-dots/A_2) integrated system (Figure 1A, curve b), E_{pa} is located at 76 mV, which is negatively shifted by 339 mV, and the corresponding cathodic peak potential is located at 6 mV. The peak-to-peak separation is calculated as 70 mV, and $E^{0\prime}$ is 41 mV, negatively shifted by 167 mV. Furthermore, this electrochemical signal is quite stable: the peak height and the peak potential remain nearly unchanged after 100 cycles (data not shown).

In addition, the CVs of poly(C-dots/A_2)-$Fe(CN)_6^{3-/4-}$ display a well-defined peak shape at different scan rates (ν), while both I_{pa} and I_{pc} increase as the scan rate, ν, is increased from 50 up to 500 mV s^{-1} (Figure 1B). The peak currents vary linearly with ν (Figure 1B, inset), whose linear regression equations are I_{pa} (μA) = 34.395 mV s^{-1} + 6.693 (R^2 = 0.991, n = 6) and I_{pc} (μA) = −32.07 mV s^{-1} − 6.313 (R^2 = 0.989, n = 6), respectively.

ECL Response. The ECL behaviors of the poly(C-dots/A_2)-$Fe(CN)_6^{3-/4-}$ were investigated in 0.05 M Tris-HCl (pH 7.4) without and with 10 mM $K_2S_2O_8$, respectively, at a scan rate of 0.1 V s^{-1} within the scan range of 0 to −1.75 V. As expected, no obvious ECL emissions can be observed on GCE/poly(C-dots/A_2)-$Fe(CN)_6^{3-/4-}$ (Figure 1C, curve a) in the absence of $K_2S_2O_8$ as a coreactant. After the addition of 10 mM $K_2S_2O_8$, an ECL emission with the peak potential located at −1.73 V appeared for GCE/poly(C-dots/A_2)-$Fe(CN)_6^{3-/4-}$ (Figure 1C, curve b). Simultaneously, the ECL responses of GCE/poly(C-dots/A_2)-$Fe(CN)_6^{3-/4-}$ obtained during a continuous potential scan display highly repeatable signals (Figure 1D), indicating good stability of the proposed ECL system.

ECL Detection of GSH. As noted above, we found accidentally that the addition of GSH could effectively quench the ECL of GCE/poly(C-dots/A_2)-$Fe(CN)_6^{3-/4-}$ as proposed in our system. Consequently, the analytical performance of the ECL sensor for GSH was evaluated. As depicted in Figure 2A, the ECL intensity of GCE/poly(C-dots/A_2)-$Fe(CN)_6^{3-/4-}$ decreased obviously with an increase in the concentration of GSH. Figure 2B presents the corresponding current, obtained as $(I_0-I)/I_0$, versus the concentration of GSH, where I_0 is the initial intensity without GSH and I is the intensity at the different concentration of GSH. The error bars represent the standard deviations based on three independent measurements. A good linear calibration plot in the concentration range of 0.1−1.0 μM with a correlation coefficient of 0.997 is displayed, and the detection limit down to 54.3 nM is obtained based on 3δ/slope (Figure 2B, inset).

The performance of the developed method for the GSH determination was compared with those recently reported in the literature (Table 1).[38−40] It appears that a comparatively high sensitivity and low detection limit can be obtained with this developed method. The enhanced analytical performance may be ascribed to the ECL quenching mechanism of GCE/poly(C-dots/A_2)-$Fe(CN)_6^{3-/4-}$ to GSH.

In order to evaluate the selectivity of this strategy for the determination of GSH, the ECL responses of the poly(C-dots/A_2)-$Fe(CN)_6^{3-/4-}$ to 10 μM of a wide range of interfering substances, including dopamine, folic acid, ascorbic acid, vitamin B_1/B_2/B_6, cysteine, alanine, methionine, tryptophan, histidine, glutamic acid, asparagic acid, and valine, were checked against GSH with the equivalent concentration. As shown in Figure 2C, no apparent ECL quenching effects are observed except for ascorbic acid and cysteine. It is worth mentioning in particular that ascorbic acid derivatives[41] and cysteine[42] could also serve as a new coreactant of ECL reactions except for peroxydisulfate and sulfite compounds. Such interference should be ascribed to the ECL quenching mechanism. However, the concentrations (μM levels) explored here are much lower than that of GSH (mM levels) in biological systems.[43−45]

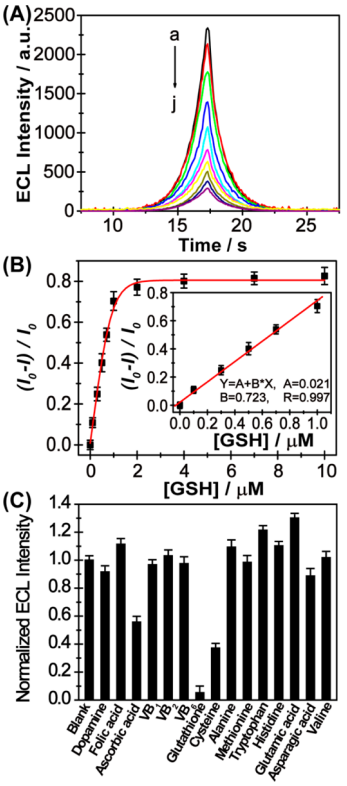

Figure 2. (**A**) ECL-time curves of poly(C-dots/A_2)-$Fe(CN)_6^{3-/4-}$ in the presence of (a−j) 0, 0.1, 0.3, 0.5, 0.7, 1, 2, 4, 7, and 10 μM GSH. The electrolyte is Tris-HCl (0.05 M, pH 7.4) with 10 mM $K_2S_2O_8$ and 0.1 M KCl. (**B**) The corresponding ECL vs GSH concentration curves. Inset: Linear calibration plot for GSH detection. (**C**) The ECL response of poly(C-dots/A_2)-$Fe(CN)_6^{3-/4-}$ in the presence of interfering substances.

Table 1. Comparison between the Developed Method and Other Reported ECL-Based Chemosensors for GSH Determination

electrode	detection range	detection limit	ref
poly(C-dots/A_2)-$Fe(CN)_6^{3-/4-}$	**0.1−1.0 μM**	**54.3 nM**	**present work**
CdSe/ZnS/Nafion	10−180 μM	1.5 μM	39
CdS_2L[a]	0.002−4 μM	0.67 nM	40
GO[b]/CdTe	24−214 μM	8.3 μM	41

[a] *N*-Hexyl-3-{2-[4-(2,2′:6′,2″-terpyridin-4′-yl)phenyl]ethenyl}-carbazole. [b] Graphene oxide.

DISCUSSION

Synergic Effect of A_2 and C-Dots. A_2 behaves the properties of a cationic surfactant. Above a critical micelle concentration (CMC), A_2 micelles can be formed from soluble surfactants, which possess regions of hydrophilic and hydro-

DOI: 10.1021/acs.analchem.5b03358
Anal. Chem. XXXX, XXX, XXX−XXX

phobic character (Scheme 1).[33] A_2 can be electropolymerized to obtain the conductive polyA_2. The irregular micelle

Scheme 1. Schematic Illustrations for A_2 Conformation at the Air−Water Interface, Micelle Structures, and the Proposed Microstructure of C-Dots/A_2

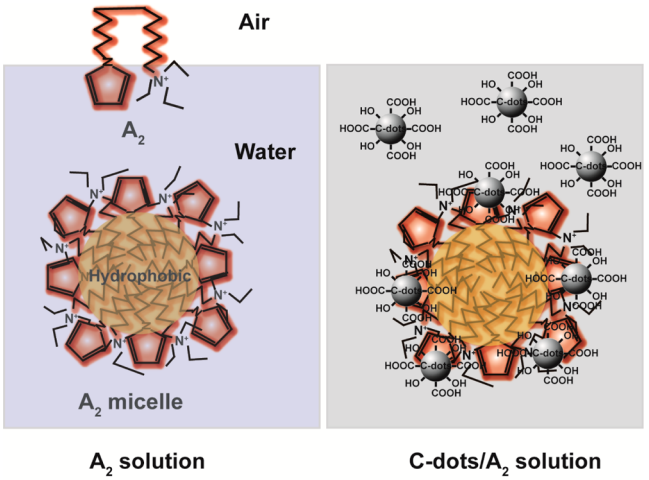

nanoparticles with the size varies from 50 to 200 nm are still observable (Figure 3A). The synthesized C-dots were of

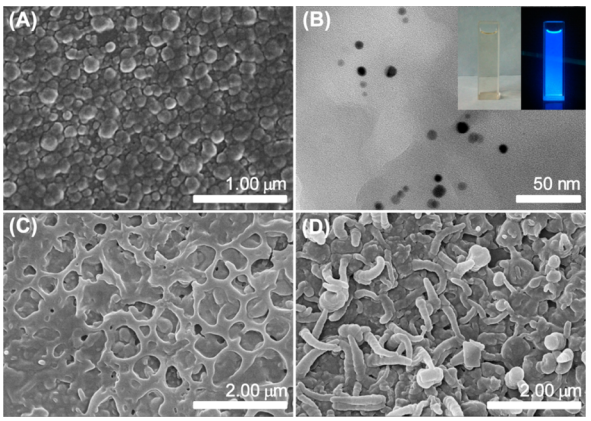

Figure 3. SEM (**A**,**C**,**D**) and TEM (**B**) images for (**A**) polyA_2, (**B**) C-dots, (**C**) poly(C-dots/A_2), and (**D**) poly(C-dots/A_2)-$Fe(CN)_6^{3-/4-}$. Inset shows the photographs of C-dots/A_2 solution under visible light (left) and under 365 nm UV light (right).

spherical shape and monodisperse NPs with particle size distribution in the range of 8 ± 2 nm (Figure 3B). Moreover, the obtained C-dots were caped with carboxyl and hydroxyl groups. The C-dots/A_2 collodial solution is pale yellow under visible light (left) but exhibits a homogeneously bright blue color under ultraviolet radiation (λ = 365 nm) (Figure 3B inset). It indicates that C-dots still maintained their fluorescent property in A_2 solution. In the uniform C-dots/A_2 collodial solution, C-dots may be loaded on the "shell" of the A_2 micelle due to the electrostatic interaction, as well as $\pi-\pi$ stacking between aromatic pyrrole end-tail group and C-dots. The hypothesized composite structure of C-dots/A_2 was illustrated in Scheme 1.

Meanwhile, as one of the pyrrole derivatives, C-dots/A_2 can be electrochemically polymerized to poly(C-dots/A_2) consecutively; while the excellent conductivity of polypyrrole can accelerate electron transfer on the electrode surface, and the immobilization of hydrophilic C-dots on the surface of GCE was achieved. For poly(C-dots/A_2), the SEM image reveals a smooth and porous film was obtained, while the particles were completely merged into the film (Figure 3C). However, compared with poly(C-dots/A_2), it can be clearly seen that rod-like particles with diameters of about 100 nm and length of about 1.5 μm were obtained for poly(C-dots/A_2)-$Fe(CN)_6^{3-/4-}$ (Figure 3D). The different morphologies revealed changes consistent with $K_4Fe(CN)_6$ and $K_3Fe(CN)_6$ being successfully confined on the surface of poly(C-dots/A_2).

The ECL Signal Amplification Mechanism of Fe-$(CN)_6^{3-/4-}$ to C-Dots. Recently, C-dots were found to exhibit excellent ECL properties similar to those of other QDs and could be used as ECL luminophores. In order to identify the luminophore and further reveal the ECL mechanism, the ECL emission spectrum of poly(C-dots/A_2)-$Fe(CN)_6^{3-/4-}$ was obtained using a fluorescence spectrometer. As displayed in Figure 4A, an emission band in the range of 450−650 nm with a maximum wavelength at 505 nm was obtained (Figure 4A, curve a). This ECL spectrum is a little red-shifted (~67 nm) compared with the C-dots fluorescence spectrum at the optimal

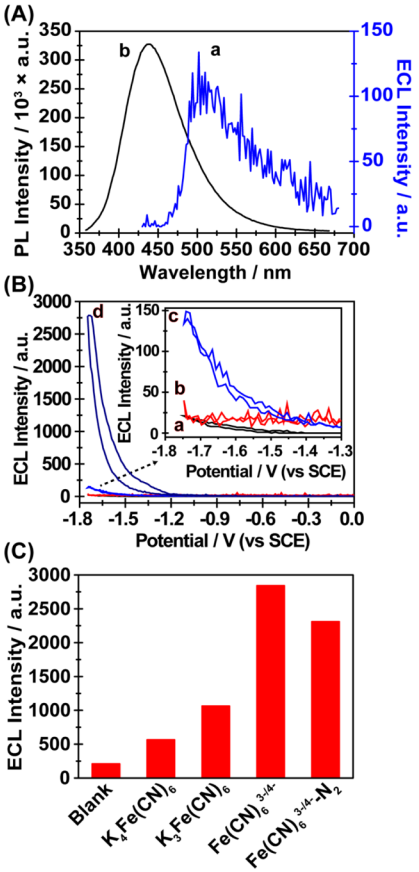

Figure 4. (**A**) ECL (a) and PL (b) spectrum of the poly(C-dots/A_2)-$Fe(CN)_6^{3-/4-}$ system. (**B**) The effect of different coreactants on the ECL intensity of poly(C-dots/A_2)-$Fe(CN)_6^{3-/4-}$: (a) O_2, (b) H_2O_2, (c) cysteine, and (d) $K_2S_2O_8$. Inset: amplification of lines a, b, and c. (**C**) ECL response of poly(C-dots/A_2), poly(C-dots/A_2)-$K_4Fe(CN)_6$, poly(C-dots/A_2)-$K_3Fe(CN)_6$, and poly(C-dots/A_2)-$Fe(CN)_6^{3-/4-}$ in Tris-HCl buffer solution (0.05 M, pH 7.4) with $K_2S_2O_8$ (10 mM) and poly(C-dots/A_2)-$Fe(CN)_6^{3-/4-}$ in Tris-HCl buffer solution (0.05 M, pH 7.4) with $K_2S_2O_8$ (10 mM) saturated by nitrogen.

DOI: 10.1021/acs.analchem.5b03358
Anal. Chem. XXXX, XXX, XXX−XXX

emission wavelengths of 438 nm (Figure 4A, curve b). The result may be explained by considering the difference in the emitting states of the ECL and fluorescence emission. It is assumed that like QDs, the ECL of C-dots is mainly produced by surface-state transitions (due to the presence of surface traps with incomplete passivation), whereas the fluorescence is more reminiscent of core states.[1−3,44] The energy band gap of surface states is smaller than that of the core states, and, therefore, the wavelength of ECL emission is higher than that of fluorescence.

The coreactant plays an important role in the production of the C-dots ECL signal since it dominantly contributes to the whole ECL process. Oxygen, hydrogen peroxide, cysteine, and $K_2S_2O_8$ are generally used as coreactants, and their effects were evaluated. As shown in Figure 4B, using O_2 or hydrogen peroxide as the coreactant, no obvious ECL signal was obtained at GCE/poly(C-dots/A_2)-Fe$(CN)_6^{3-/4-}$ (Figure 4B, curve a,b). However, a weak cathodic ECL signal was realized when cysteine served as the coreactant (Figure 4B, curve c), and a strong cathodic ECL signal was obtained when $K_2S_2O_8$ was added and reacted with the proposed ECL sensor (Figure 4B, curve d). It indicates that the ECL mechanism is partially similar to most of the C-dots following the cathodic ECL mechanism using $K_2S_2O_8$ as the coreactant:[11] the functional oxygen-containing groups of C-dots facilitate the electrogeneration of C-dots$^{\bullet-}$ radicals, meanwhile strongly oxidizing $SO_4^{\bullet-}$ radicals are produced by electrochemical reduction of $S_2O_8^{2-}$. Subsequently, C-dots$^{\bullet-}$ radicals can react with $SO_4^{\bullet-}$ radicals via electron-transfer annihilation to form the excited-state (C-dots*) for ECL emission.

Furthermore, we investigated the effects of the confined Fe$(CN)_6^{3-/4-}$ on the ECL of the immobilized C-dots using $S_2O_8^{2-}$ as the coreactant. As described in Figure 4C, only a weak ECL signal can be obtained at GCE/poly(C-dots/A_2). The presence of Fe$(CN)_6^{3-}$ or Fe$(CN)_6^{4-}$ results in the increased ECL signal. The dramatically enhanced ECL signal (10 times higher) can be produced at GCE/poly(C-dots/A_2)-Fe$(CN)_6^{3-/4-}$. It indicates that the amplified ECL may be induced by the Fe$(CN)_6^{3-/4-}$ redox couple. The excited-state C-dots can result from annihilation of electron-injected and hole-injected C-dots produced by a series of possible reactions. Ferricyanide can serve as the hole- injector and convert C-dots to C-dot$^{\bullet+}$.[46] Besides, when the ECL experiments are carried out in nitrogen-saturated solution, poly(C-dots/A_2)-Fe$(CN)_6^{3-/4-}$ shows a little ECL intensity decrease, indicating that oxygen is a necessary reactive intermediate for ECL generation.

Cyclic voltammetry (CV) is often used to study a variety of redox processes, to determine the stability of reaction products, the presence of intermediates in redox reactions, reaction and electron transfer kinetics, and the reversibility of reaction. Thus, the designed CV experiments were performed to study the electrochemical action of dissolved O_2 and reveal the enhancing effect of O_2 for the proposed ECL system. CVs of GCE/poly(C-dots/A_2) and GCE/poly(C-dots/A_2)-Fe$(CN)_6^{3-/4-}$ recorded in 0.05 M Tris-HCl buffer solution (pH 7.4) containing 0.1 M KCl were shown in Figure 5A and Figure 5B, respectively. The redox signal of the confined Fe$(CN)_6^{3-/4-}$ can be well distinguished (Figure 5B, curve a). In the presence of O_2, the anodic and cathodic peak current of this redox signal increase simultaneously (Figure 5B, curve b). The reactions of ferric with reducing agents are well-known. Oxygen, when present, gets reduced via superoxide anion, hydrogen peroxide, and hydroxyl radical to water.[47] Thus, at GCE/poly(C-dots/

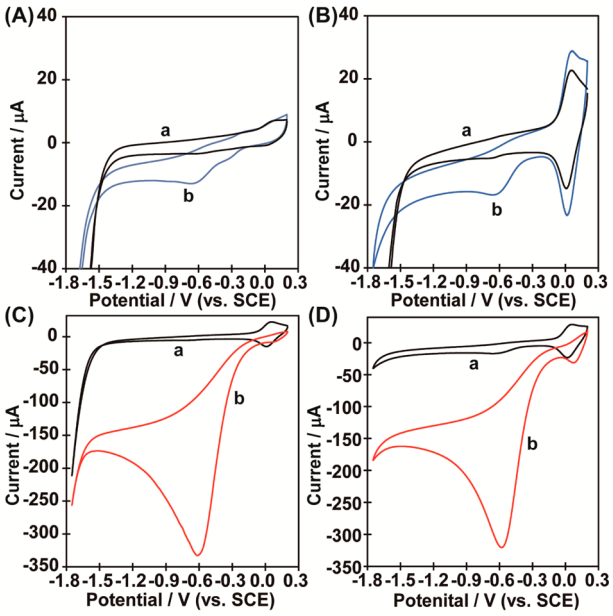

Figure 5. CVs of the modified electrodes recorded in 0.1 M PBS (pH 7.0) for (**A**) GCE/poly(C-dots/A_2) in the absence (a) and presence of O_2 (b), (**B**) GCE/poly(C-dots/A_2)-Fe$(CN)_6^{3-/4-}$ in the absence (a) and presence of O_2 (b), (**C**) under N_2, GCE/poly(C-dots/A_2)-Fe$(CN)_6^{3-/4-}$ in the absence (a) and presence of 10 mM $K_2S_2O_8$ (b), (**D**) under ambient atmosphere, GCE/poly(C-dots/A_2)-Fe$(CN)_6^{3-/4-}$ in the absence (a) and presence of 10 mM $K_2S_2O_8$ (b).

A_2)-Fe$(CN)_6^{3-/4-}$, O_2 can be converted into $O_2^{\bullet-}$ by Fe$(CN)_6^{4-}$. The phenomenon of this autocatalysis may be thus ascribed to the following equations:

$$Fe(CN)_6^{3-} + e \rightarrow Fe(CN)_6^{4-} \quad (1)$$

$$O_2 + Fe(CN)_6^{4-} \rightarrow O_2^{\bullet-} + Fe(CN)_6^{3-} \quad (2)$$

$$C\text{-dot} + O_2^{\bullet-} \rightarrow C\text{-dot}^{\bullet-} + O_2 \quad (3)$$

The effect of O_2 on the CV response of GCE/poly(C-dots/A_2)-Fe$(CN)_6^{3-/4-}$ to 10 mM $K_2S_2O_8$ was also evaluated. In the absence of O_2, Fe$(CN)_6^{3-}$ was reduced into Fe$(CN)_6^{4-}$ directly: the anodic peak current decreased as no more decrement was observed for the cathodic peak current (Figure 5C). Differently, in the presence of O_2, the typical electrocatalysis phenomenon can be also observed: anodic peak currents decrease with increment of the cathodic peak current (Figure 5D). It indicates that reduction of $S_2O_8^{2-}$ can be electrocatalyzed by Fe$(CN)_6^{3-/4-}$ in the presence of O_2. Consequently, as illustrated in Scheme 2, the Fe$(CN)_6^{3-/4-}$ induced ECL signal amplification mechanism of C-dots was proposed as the following equations:

$$C\text{-dot} + e \rightarrow C\text{-dot}^{\bullet-} \quad (4)$$

$$C\text{-dot} + Fe(CN)_6^{3-} \rightarrow C\text{-dot}^{\bullet+} + Fe(CN)_6^{4-} \quad (5)$$

$$C\text{-dot}^{\bullet+} + C\text{-dot}^{\bullet-} \rightarrow C\text{-dot}^{*} \quad (6)$$

$$S_2O_8^{2-} + Fe(CN)_6^{4-} \rightarrow SO_4^{2-} + SO_4^{\bullet-} + Fe(CN)_6^{3-} \quad (7)$$

$$C\text{-dot}^{\bullet-} + SO_4^{\bullet-} \rightarrow C\text{-dot}^{*} + SO_4^{2-} \quad (8)$$

$$C\text{-dot}^{*} \rightarrow C\text{-dot} + h\nu\ (\sim 505\ nm) \quad (9)$$

DOI: 10.1021/acs.analchem.5b03358
Anal. Chem. XXXX, XXX, XXX−XXX

Scheme 2. Schematic Diagrams for the ECL Reaction Mechanism of the Poly(C-dots/A_2)-Fe$(CN)_6^{3-/4-}$-$S_2O_8^{2-}$/O_2 System

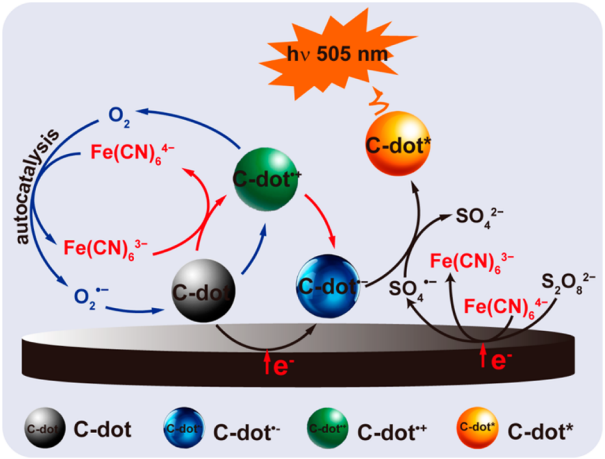

ECL Quenching Mechanism of Poly(C-dots/A_2)-Fe$(CN)_6^{3-/4-}$ by GSH. It is well-known that GSH exerts its properties as an antioxidant due to the reactivity of the sulfhydryl groups; therefore, it is evident that the reaction of sulfhydryl groups with $SO_4^{\bullet-}$ would impede the radiative recombination of electrons and holes trapped on the C-dots surface, causing the ECL quenching of the proposed sensor.[38] The probable quenching mechanism was proposed as the following equations:

$$SO_4^{\bullet-} + R{-}SH + OH^- \rightarrow R{-}S^{\bullet} + SO_4^{2-} + H_2O \quad (10)$$

$$R{-}S^{\bullet} + R{-}S^{\bullet} \rightarrow R{-}S{-}S{-}R \quad (11)$$

In addition, this explanation demonstrates as well that the interference of cysteine and ascorbic acid is due to their similar inhibition to $S_2O_8^{2-}$. However, the other interfering agents investigated have no analogous unit and cannot serve as a coreactant to compete with $K_2S_2O_8$ in GSH determination. Therefore, the ECL sensor for GSH determination demonstrates excellent selectivity and exhibits a favorable anti-interference property toward common disruptors in a biological environment.

CONCLUSION

In conclusion, we have developed an ECL pathway of C-dots with the participation of Fe$(CN)_6^{3-/4-}$, which facilitated C-dots oxidation and expeditiously converted $S_2O_8^{2-}$ to $SO_4^{\bullet-}$, forming a high yield of C-dot*. Furthermore, amplification methodology could improve the shortcomings of C-dots ECL, such as low emission efficiency and unstable radical species. We used the as-prepared ECL platform to realize the sensitive and selective detection of glutathione in the presence of other interfering substances. This work improved C-dots ECL technology, expanded its signal amplification strategy, and predicted the potential abilities of C-dots in analytical methodologies.

AUTHOR INFORMATION

Corresponding Author

*Fax: 86-25-84303107. E-mail: danshan@njust.edu.cn, danshan@yzu.edu.cn.

Notes

The authors declare no competing financial interest.

ACKNOWLEDGMENTS

This research was supported by National Natural Science Foundation of China (Grant No. 21175114), Qing Lan project of Jiangsu Province, the Fundamental Research Funds for the Central Universities (30915015101, 30920130112012, 30920140112009), and a project founded by the priority academic program development of Jiangsu Higher Education Institutions.

REFERENCES

(1) Baker, S. N.; Baker, G. A. *Angew. Chem., Int. Ed.* **2010**, *49*, 6726–6744.
(2) Georgakilas, V.; Perman, J. A.; Tucek, J.; Zboril, R. *Chem. Rev.* **2015**, *115*, 4744–4822.
(3) Krysmann, M. J.; Kelarakis, A.; Dallas, P.; Giannelis, E. P. *J. Am. Chem. Soc.* **2012**, *134*, 747–750.
(4) Sun, Y.; Zhou, B.; Lin, Y.; Wang, W.; Fernando, K. A. S.; Pathak, P.; Meziani, M. J.; Harruff, B. A.; Wang, X.; Wang, H.; Luo, P.; Yang, H.; Kose, M. E.; Chen, B.; Veca, L. M.; Xie, S. *J. Am. Chem. Soc.* **2006**, *128*, 7756–7757.
(5) Guo, X.; Wang, C. F.; Yu, Z.; Chen, L.; Chen, S. *Chem. Commun.* **2012**, *48*, 2692–2694.
(6) Li, X.; Liu, Y.; Song, X.; Wang, H.; Gu, H.; Zeng, H. *Angew. Chem., Int. Ed.* **2015**, *54*, 1759–1764.
(7) Qu, S.; Wang, X.; Lu, Q.; Liu, X.; Wang, L. *Angew. Chem.* **2012**, *124*, 12381–12384.
(8) Li, W.; Zhang, Z.; Kong, B.; Feng, S.; Wang, J.; Wang, L.; Yang, J.; Zhang, F.; Wu, P.; Zhao, D. *Angew. Chem., Int. Ed.* **2013**, *52*, 8151–8155.
(9) Ding, C.; Zhu, A.; Tian, Y. *Acc. Chem. Res.* **2014**, *47*, 20–30.
(10) Liu, C.; Zhang, P.; Zhai, X.; Tian, F.; Li, W.; Yang, J.; Liu, Y.; Wang, H.; Wang, W.; Liu, W. *Biomaterials* **2012**, *33*, 3604–3613.
(11) Xu, Y.; Liu, J.; Gao, C.; Wang, E. *Electrochem. Commun.* **2014**, *48*, 151–154.
(12) Zheng, L.; Chi, Y.; Dong, Y.; Lin, J.; Wang, B. *J. Am. Chem. Soc.* **2009**, *131*, 4564–4565.
(13) Li, L.; Ji, J.; Fei, R.; Wang, C.; Lu, Q.; Zhang, J.; Jiang, L.; Zhu, J. *Adv. Funct. Mater.* **2012**, *22*, 2971–2979.
(14) Zhang, P.; Xue, Z.; Luo, D.; Yu, W.; Guo, Z.; Wang, T. *Anal. Chem.* **2014**, *86*, 5620–5623.
(15) Wu, L.; Wang, J.; Ren, J.; Li, W.; Qu, X. *Chem. Commun.* **2013**, *49*, 5675–5677.
(16) Yang, S.; Liang, J.; Luo, S.; Liu, C.; Tang, Y. *Anal. Chem.* **2013**, *85*, 7720–7725.
(17) Long, Y.; Bao, L.; Zhao, J.; Zhang, Z.; Pang, D. *Anal. Chem.* **2014**, *86*, 7224–7228.
(18) Dang, J.; Guo, Z.; Zheng, X. *Anal. Chem.* **2014**, *86*, 8943–8950.
(19) Swanick, K. N.; Hesari, M.; Workentin, M. S.; Ding, Z. *J. Am. Chem. Soc.* **2012**, *134*, 15205–15208.
(20) Hesari, M.; Workentin, M. S.; Ding, Z. *ACS Nano* **2014**, *8*, 8543–8553.
(21) Wu, P.; Hou, X.; Xu, J.; Chen, H. *Chem. Rev.* **2014**, *114*, 11027–11059.
(22) Dong, Y.; Gao, T.; Zhou, Y.; Zhu, J. *Anal. Chem.* **2014**, *86*, 11373–11379.
(23) Lv, X.; Pang, X.; Li, Y.; Yan, T.; Cao, W.; Du, B.; Wei, Q. *ACS Appl. Mater. Interfaces* **2015**, *7*, 867–872.
(24) Deng, S.; Lei, J.; Huang, Y.; Cheng, Y.; Ju, H. *Anal. Chem.* **2013**, *85*, 5390–5396.
(25) Liu, Z.; Qi, W.; Xu, G. *Chem. Soc. Rev.* **2015**, *44*, 3117–3142.
(26) Ye, H.; Xu, H.; Xu, X.; Zheng, C.; Li, X.; Wang, L.; Liu, X.; Chen, G. *Chem. Commun.* **2013**, *49*, 7070–7072.
(27) Zhang, H.; Han, Z.; Wang, X.; Li, F.; Cui, H.; Yang, D.; Bian, Z. *ACS Appl. Mater. Interfaces* **2015**, *7*, 7599–7604.

DOI: 10.1021/acs.analchem.5b03358
Anal. Chem. XXXX, XXX, XXX–XXX

(28) Xu, S.; Liu, Y.; Wang, T.; Li, J. *Anal. Chem.* **2011**, *83*, 3817−3823.
(29) Deng, S.; Hou, Z.; Lei, J.; Lin, D.; Hu, Z.; Yan, F.; Ju, H. *Chem. Commun.* **2011**, *47*, 12107−12109.
(30) Lei, J.; Ju, H. *Chem. Soc. Rev.* **2012**, *41*, 2122−2134.
(31) Yin, M.; Wu, L.; Li, Z.; Ren, J.; Qu, X. *Nanoscale* **2012**, *4*, 400−404.
(32) Wang, J.; Zhao, W.; Li, X.; Xu, J.; Chen, H. *Chem. Commun.* **2012**, *48*, 6429−6431.
(33) Deng, S.; Zhang, T.; Shan, D.; Wu, X.; Dou, Y.; Cosnier, S.; Zhang, X. *ACS Appl. Mater. Interfaces* **2014**, *6*, 21161−21166.
(34) Ding, S.; Chen, J.; Xia, J.; Wang, Y.; Cosnier, S. *Electrochem. Commun.* **2013**, *34*, 339−343.
(35) Chen, C.; Liu, W.; Xu, C.; Liu, W. *Biosens. Bioelectron.* **2015**, *71*, 68−74.
(36) Dennany, L.; Gerlach, M.; O'Carroll, S.; Keyes, T. E.; Forster, R. J.; Bertoncello, P. *J. Mater. Chem.* **2011**, *21*, 13984−13990.
(37) Niu, W.; Li, Y.; Zhu, R.; Shan, D.; Fan, Y.; Zhang, X. *Sens. Actuators, B* **2015**, *218*, 229−236.
(38) Xu, C.; Li, H.; Yin, B. *Biosens. Bioelectron.* **2015**, *72*, 275−281.
(39) Zhang, C.; Wang, Lei.; Zhang, S.; Mao, C.; Song, J.; Niu, H.; Jin, B.; Tian, Y. *Anal. Methods* **2015**, *7*, 1395−1400.
(40) Wang, Y.; Lu, J.; Tang, L.; Chang, H.; Li, J. *Anal. Chem.* **2009**, *81*, 9710−9715.
(41) Yuan, Y.; Li, H.; Han, S.; Hu, L.; Parveena, S.; Xu, G. *Anal. Chim. Acta* **2011**, *701*, 169−173.
(42) Dong, Y.; Tian, W.; Ren, S.; Dai, R.; Chi, Y.; Chen, G. *ACS Appl. Mater. Interfaces* **2014**, *6*, 1646−1651.
(43) Saha, A.; Jana, N. R. *Anal. Chem.* **2013**, *85*, 9221−9228.
(44) Lin, Z.; Xue, W.; Chen, H.; Lin, J. *Anal. Chem.* **2011**, *83*, 8245−8251.
(45) Amelia, M.; Lincheneau, C.; Silvi, S.; Credi, A. *Chem. Soc. Rev.* **2012**, *41*, 5728−5743.
(46) Amjadi, M.; Manzoori, J. L.; Hallaj, T.; Sorouraddin, M. H. *Spectrochim. Acta, Part A* **2014**, *122*, 715−720.
(47) Zomer, B.; Collé, L.; Jedyńska, A.; Pasterkamp, G.; Kooter, I.; Bloemen, H. *Anal. Bioanal. Chem.* **2011**, *401*, 2945−2954.

DOI: 10.1021/acs.analchem.5b03358
Anal. Chem. XXXX, XXX, XXX−XXX